Optical properties of silicon nanopillars with a built-in vertical $p-n$-junction

© L.S. Basalaeva[1], A.V. Tsarev[1,2], K.V. Anikin[1], S.L. Veber[2,3], N.V. Kryzhanovskaya[4], Yu.V. Nastaushev[1]

[1] Rzhanov Institute of Semiconductor Physics, Siberian Branch, Russian Academy of Sciences,
630090 Novosibirsk, Russia
[2] Novosibirsk State University,
630090 Novosibirsk, Russia
[3] International Tomography Center, Siberian Branch of Russian Academy of Sciences,
630090 Novosibirsk, Russia
[4] Alferov Federal State Budgetary Institution of Higher Education and Science
Saint Petersburg National Research Academic University of the Russian Academy of Sciences,
194021 St. Petersburg, Russia

E-mail: basalaeva@isp.nsc.ru

Received November 10, 2021
Revised November 20, 2021
Accepted November 20, 2021

Resonance reflection of light from the ordered arrays of silicon nanopillars (Si NP) was investigated. The height of Si NP was 450 nm. The effect of Si NP oxidation in concentrated nitric acid on the position of resonances in reflection spectra was studied. A weak influence of the additional polymeric coating on the characteristics of reflection from the structures was proven. It is established on the basis of the results of experimental investigation and direct numerical modeling by means of three-dimensional finite difference time domain algorithm (3D FDTD) that the dependence of the resonant wavelength for Si NP on the diameter of Si NP is a linear function with nonzero displacement depending on the pitch.

Keywords: silicon nanopillars, structural colors, all-dielectric nanophotonics.

DOI: 10.21883/SC.2022.03.53067.9761

1. Introduction

Future development of the state-of-the-art nanophotonics is closely linked with the investigations of optical properties of metal and dielectric nanostructures [1–5]. As opposed to plasmonic nanoobjects, dielectric nanoparticles are characterized by strong optically-induced magnetic dipole resonance and low loss [6]. Spherical silicon nanoparticles with typical sizes from 100 to 200 nm demonstrate strong magnetic dipole resonance in the visible spectrum [7]. The researchers were initially interested in the most simple version of silicon nanoparticles — nanospheres. It should be noted that with the development of semiconductor technology, the shape and arrangement of the nanoobjects of interest may become more complicated within a wide size range [8]. However, silicon nanopillars (Si NP) are still the most important and understudied subject of research. Unusual optical and electrical properties of Si NP are investigated in order to implement new space-saving Si NP-based devices in various applications: photovoltaics [9], nanosensorics [10] and color printing [11,12]. Structural color of dielectric nanoobject assemblies is a very interesting and useful phenomenon for various photon applications. It is important that the same material may have a different color, when its surface is nanostructured in different ways. Organic dye and pigments widely used as filters have a set of significant disadvantages: resolution restrictions, degradation with time, insufficient intensity level etc. Prototypes of reflecting and transmission color filters based on Si nanodisks and nanopillars with low aspect ratio p ($p=$ height/diameter) have been already developed [13–15]. The interest in high-aspect Si NP is directly associated with the investigations carried out in order to improve the solar cell performance [16]. Decreased reflectance is directly associated with the increased Si NP length [17].

Si NP with a height of 450 nm with vertical internal $p-n$-junction was investigated here. This paper follows our investigations. In [18], we demonstrated that such Si NP with vertical internal $p-n$-junction have a selective photoresponse. Spectral features of structural photoresponse may be controlled by choosing certain properties and array of Si NP. In spite of a great number of studies of optical properties of Si NP, Si NP with vertical $p-n$-junction have been still understudied. Si NP with radial $p-n$-junction are used more widely. It shall be noted that structures with vertical $p-n$-junction can be introduced more easily into the current manufacturing of thin-film silicon solar cells [19]. A Si NP square lattice is investigated herein for the following reasons. This is the most popular of the array arrangement forms. Only deep understanding of properties of the simplest Si NP system will enable the achievement of more complicated Si NP shapes and array geometry. Experimental and theoretical research has shown that lattice resonances occurred in the reflection spectra from Si NP square arrays (for example, see [20]). When considering optical properties of single Si NP or Si NP arrays with a pitch greater that the incident wavelength, features associated with the radial mode are focused. The influence of height on the optical properties

distribution was studied to a lesser extent. A recent paper [21] showed that longitudinal modes excited in Si NP influence the light absorption resonance position in Si NP. In [21], separation of radial and longitudinal resonances and prevailing Mie resonances in the presence of light absorption are reported. The findings described in our paper prove the conclusions in [21] regarding the prevailing Mie resonances since the visible light absorption in silicon may be increased in epitaxial structures with $p-n$-junction. In addition, dependence of optical resonances vs. pitch and diameter of Si NP with vertical $p-n$-junction is investigated herein.

2. Experiment

Si NP were formed on an initial $\langle 100 \rangle$ substrate by means of reactive ion etching via a negative electron resist mask. The silicon substrate had a $p-n$-junction that constituted epitaxial structures grown using a molecular beam epitaxy method. On the silicon (100) surface at 700°C, a 100 nm buffer silicon layer was grown above which a heavily boron compound-doped 100 nm p-type silicon layer was grown at 500°C. Si NP microarrays were patterned on this substrate by means of scanning electron lithography on a negative resist with subsequent reactive ion etching. For the detailed description of our patterning procedure see [18,22,23]. It is important that no metal mask is used for structuring, since metal dopes silicon. Si NP microarrays with a diameter from 150 to 280 nm, a height of 0.45 μm, a pitch of 400, 600, 700, 800, 900, and 1000 nm were formed. After etching, a slight polymer coating remained on the walls — a film with a thickness up to 20 nm. During etching, passivating coating is deposited on the structure walls to ensure additional protection of the side walls. Figure 1 shows a Si NP image obtained using a scanning electron microscopy (SEM image) immediately after etching. Additional passivating coating is deposited during etching, but is considered as transparent for optical emission within 400–900 nm. Experimental measurements of reflection spectra were carried out before and after removal of the coating. The coating was removed by boiling Si NP samples in concentrated nitric acid. Figure 2 shows SEM images of Si NP after boiling in concentrated nitric acid: Fig. 2, *a* is an image without Y axis correction, Fig. 2, *b* is an image with Y axis correction. Figure A.1 (*Appendix*) shows additional SEM images explaining the features of Y axis size correction. The formed Si NP microarrays demonstrated different color — structural color. Figure A.2 (*Appendix*) shows optical images of some Si NP arrays in bright field (Fig. A.2, *a*) and dark field (Fig. A.2, *b*). Size of each square array is $40 \times 40\,\mu$m. The caption of Fig. A.2 contains Si NP diameters measured including polymer coating with diameter without polymer coating given in brackets. Diameter measurement accuracy was $\pm 5-7$ nm. Reflection angles of Si NP microarrays were measured using Hyperion 2000 microscope combined with Bruker Vertex 80v FT-IR spectrometer. A 40x, NA = 0.45 objective lens was used for the measurements. The signal was normalized by the silicon slice signal. Numerical calculation of the microarray reflection spectra was carried out using Rsoft FullWave software package [24] using 3D finite difference time domain (3D FDTD) and periodic boundary conditions for a single Si NP [21]. The calculation was focused on normal incidence and reflection of linearity polarized light as well as absorption in NP.

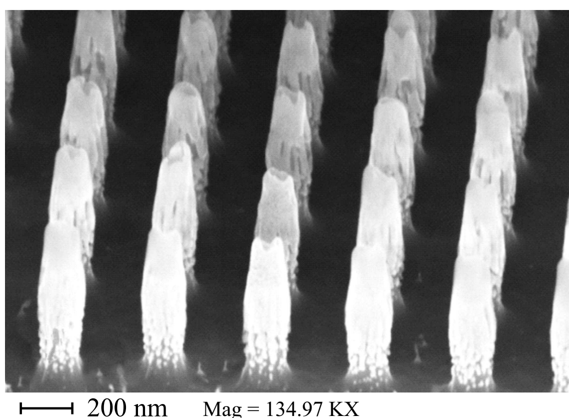

Figure 1. SEM image of Si NP array with a pitch of 400 nm after etching with polymer coating on the walls (slope angle is 54° with Y axis correction, 200 nm scale bar).

3. Experimental results

Earlier in [18], similar Si NP structures were formed with similar geometry. On the walls of these Si NP, an additional polymer layer was formed during etching, and this layer was not removed before optical measurements and the diameter was measured including the layer. Real Si NP diameter without the layer was not specified in our paper [18]. The purpose of the investigation was to define whether the layer influences the optical emission reflection or not. Si NP microarrays were formed experimentally and reflection spectra were measured before and after boiling in concentrated nitric acid. Figure 3 shows reflection spectra for Si NP microarrays with a pitch of 500 and 600 nm obtained before and after boiling in nitric acid. It is apparent that the spectra almost coincide. Thus, the additional polymer coating remaining after etching has a negligible influence on the optical resonances of structures.

The experimentally measured reflection spectra recorded one deep minimum that was in strong dependence on the Si NP diameter and one small minimum that was in low dependence on the Si NP diameter which is clearly shown in Fig. 4. This was outlined in our paper [18], but the nature of these minima was not explained. Numerical simulation shows that occurrence of additional minima in the reflection signal whose positions do not depend on the Si NP diameter may be attributable to a periodic structure resonance scattering at wavelength λ equal to its pitch (Λ) or to the interference of light waves reflected from NP boundaries and free surface (between NP).

Figure 4, *a* shows a reflection spectrum for Si NP microarrays with a pitch of 400 nm and different diameters.

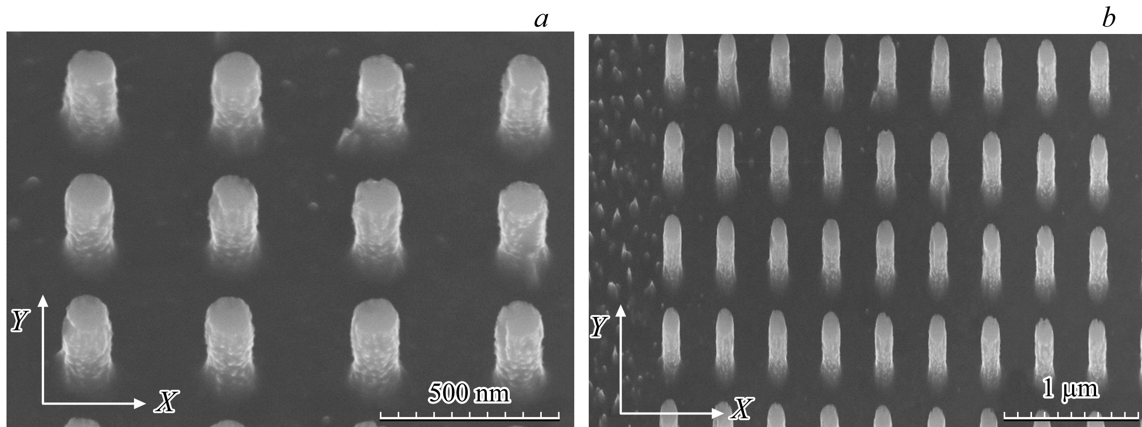

Figure 2. SEM image of Si NP with a pitch of 400 nm after boiling in HNO_3, slope angle is 30°: *a* — without *Y* axis correction; *b* — with *Y* axis correction.

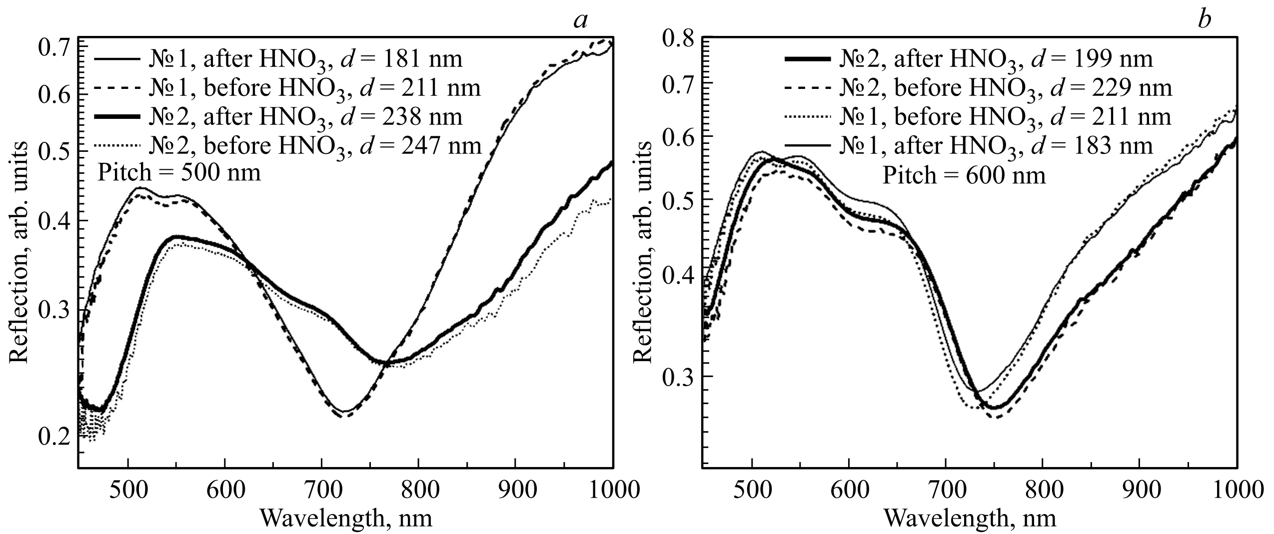

Figure 3. Reflection spectra before and after boiling in nitric acid for Si NP with an array pitch of 500 (*a*) and 600 nm (*b*).

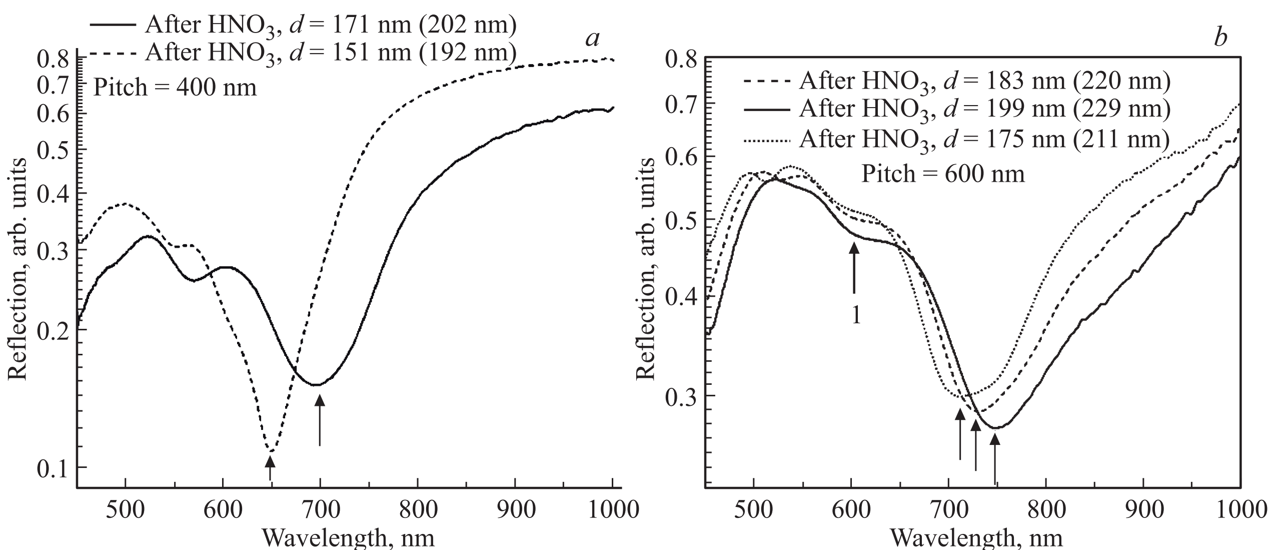

Figure 4. *a* — reflection spectra of Si NP microarrays with a pitch of 400 nm (Si NP diameter is 171 and 151 nm) after boiling in nitric acid; *b* — reflection spectra of Si NP microarrays with a pitch of 600 nm (Si NP diameter is 175, 183, 199 nm) after boiling in nitric acid. In the detail in brackets, an Si NP diameter is given that was measured with an additional polymer coating before boiling in nitric acid. Black arrows show the radial mode position, arrow № 1 shows resonance $\lambda = \Lambda$ (Λ is a square lattice pitch).

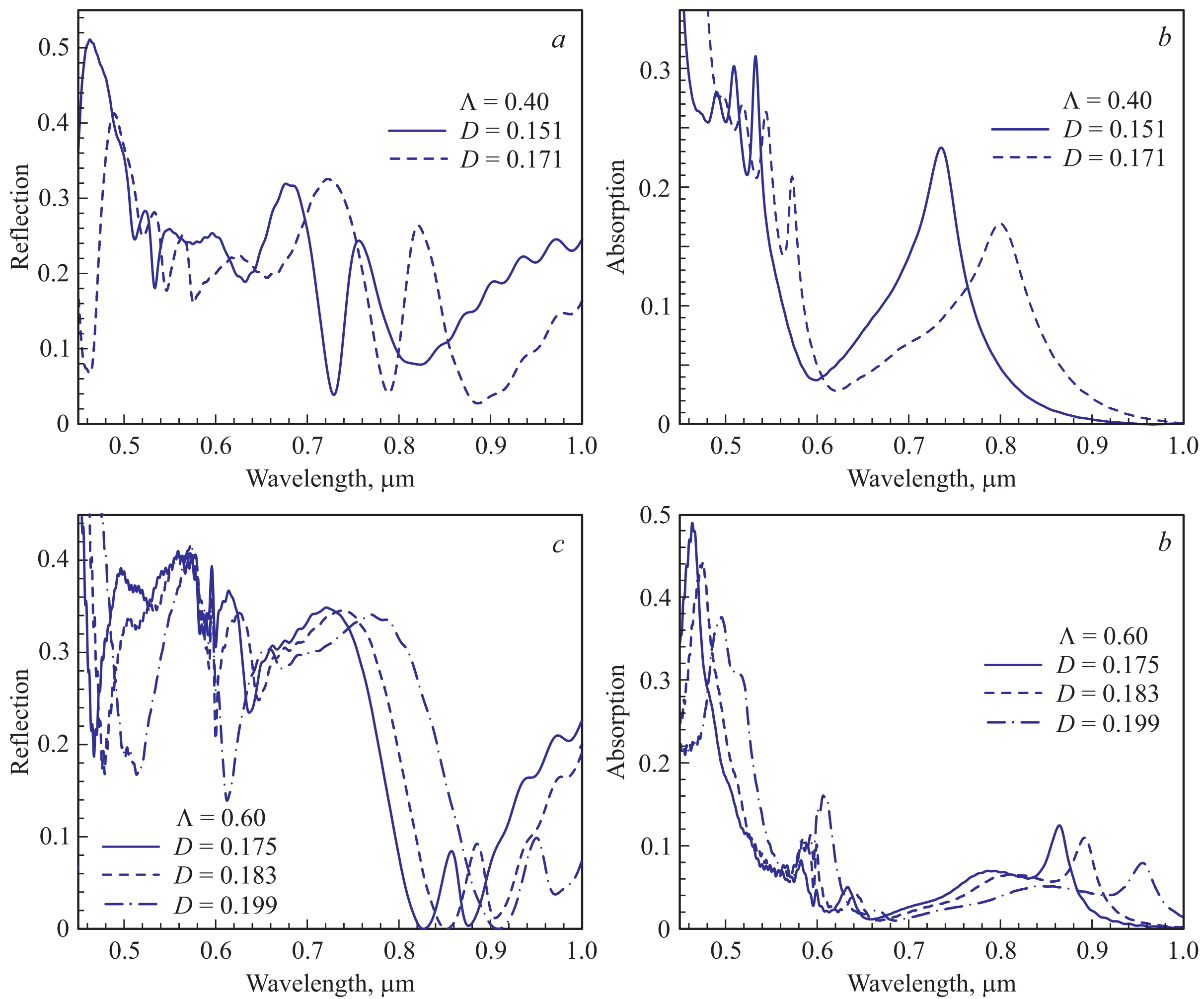

Figure 5. Calculated reflection spectra (a, c) and absorption spectra (b, d) of optical wave from NP shown in Fig. 2, *a* and *b*.

The black arrow shows the minimum that depends strongly on the diameter and moves into a long-wave region, when the Si NP diameter is increased. However, for structures with a pitch of 600 nm (see Fig. 4, *b*), a weak minimum is observed (in a short-wave region) that is shown with arrow № 1 and that does not depend on the Si NP diameter as specified above.

Figure 4, *b* shows that the main minimum position (shown with small black arrows) strongly depends on the diameter and moves into a long-wave region with the increase in the Si NP diameter.

4. Numerical simulation of Si NP reflection and absorption spectra

In order to explain the nature of the observed experimental minima, numerical simulation of the Si NP reflection and absorption spectral characteristics was performed. Figure 5 shows calculated reflection and absorption spectra for the optical wave from the Si NP microarrays.

It shall be noted that the Si NP reflection spectra have fundamental differences from the experimental spectra that shall be explained. In the Si NP reflection spectra, we observe the interference of optical waves reflected from a free surface and reradiated Si NP waves. These waves are summed up in opposition when the reflection signal minimum is formed.

The energy of the wave reflected from the free surface at the nanopillar base depends on the reflectance and relative area:

$$S_D = \frac{4\Lambda^2}{\pi D^2} - 1,$$

where Λ is the nanopillar pitch in the square lattice, D is the Si NP diameter. For the free surface, the reflectance is in small dependence from the wavelength and is equal to ~ 0.4. For experimental structures, it may significantly differ due to increased surface roughness after Si NP etching. SEM images of experimentally formed structures show that the free silicon surface near Si NP is characterized by significant etching roughness (see Figs. 1 and 2). Contribution of a scattered wave from Si NP may be higher or lower than the contribution of the reflection from the free surface. When the pitch is rather large, then the contribution from the free surface is always

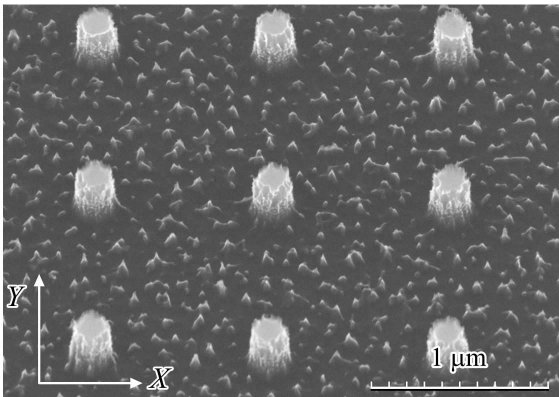

Figure 6. SEM image of Si NP with a pitch of 1000 nm, slope angle 30°, without Y axis correction.

governing, therefore a single main minimum is always observed in a large-pitch structures, which is observed both in the experiment and calculation. In addition, for our experimentally formed structures, large-pitch Si NP are characterized by a significant increase in the silicon surface roughness. Figure 6 shows a SEM image of Si NP with a pitch of 1000 nm. In this case, it can be observed that the silicon surface roughness between Si NP is significantly higher than for Si NP with a pitch of 400 nm (Fig. 2, *a*).

For structures with a small pitch, contribution of scattering from Si NP may exceed the contribution from the free surface. Contribution from Si NP may be evaluated using a wave energy absorbed within Si NP itself (due to significant virtual component of the silicon refraction index in the visible spectrum). In addition, the contribution of nanopillars in the experiment can significantly differ from the calculated one due to additional scattering sources on NP interface discontinuities as well as due to additional absorption on the internal $p-n$-junction.

Thus, it is preferable to compare with the experiment of our structures based on the calculated absorption spectra of Si NP that are shown in Fig. 5, *b* and *d*. An absorption peak is observed in 0.6–0.9 μm spectral region of interest. In the spectrum maximum region, contribution from Si NP exceeds the contribution of scattering from the free surface and a local maximum is observed in the calculated reflectance dependences whose position corresponds to the maximum in the reflectance spectrum. When the measured wavelength deflects from the maximum position, the reflected energy amplitude is gradually decreased, crosses zero and then again begins to rise. This is the reason why two minima in the reflection spectrum are observed for several small-pitch structures. Therefore, as mentioned above, calculation of the Si NP optical wave absorption spectrum shall be preferably used for correct analysis of such structures.

In our experimental conditions, scattering power from Si NP and reflection power from the mirror surface differ greatly and no contribution matching conditions are observed. Therefore, on Fig. 4, only one main minimum is observed. Thus, the difference in data in Figs. 4 and 5 is not an experimental or calculation error and is a consequence of changed surface properties of silicon and NP (increased roughness) after preparation of Si NP during selective etching.

It shall be noted that the use of smaller geometrical sizes is more advantageous than those that were used in our experiments (see Fig. 7) due to the existing technological constraints. For small sizes, high contribution of scattering from NP is observed (see Fig. 7) which is characterized by deep single minima of reflected power and high absorption level of NP. In combination with the internal $p-n$-junction, this will give a high photoresponse level with a spectral peak defined by the NP diameter. It shall be noted that our calculations are well correlated with the similar data obtained earlier by means

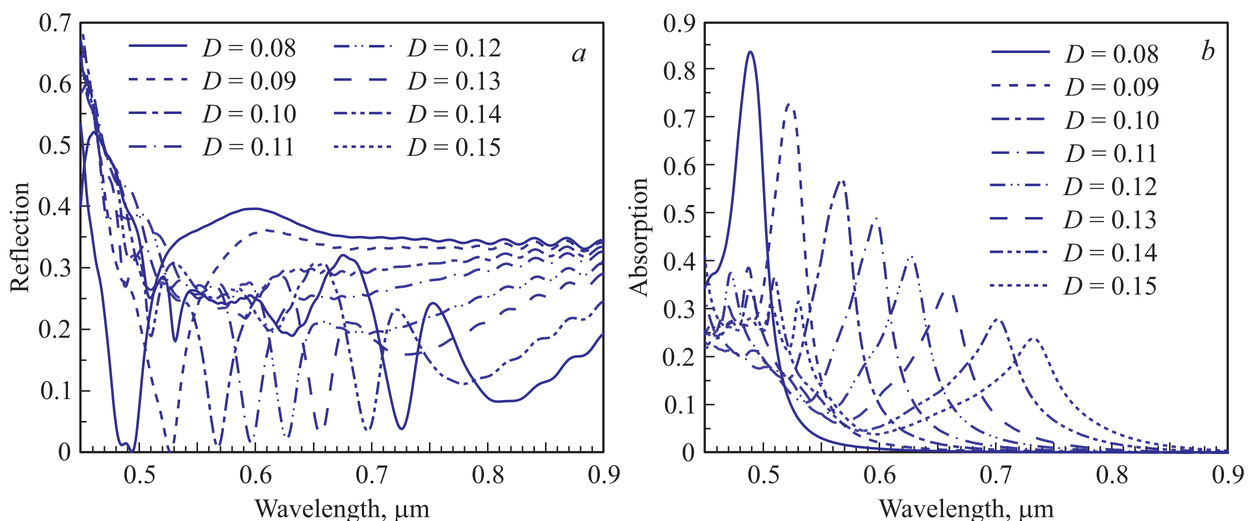

Figure 7. Calculated reflection (*a*) and absorption (*b*) spectra of the optical wave from small diameter NP for pitch $\Lambda = 0.4\,\mu$m.

of experiment and calculation for NP with a diameter of 80 nm [21].

5. Mie resonance observance condition and evaluation of coefficient K

A calculation method may be used for simple evaluation of minima positions in the Si NP reflection spectra. Generally, for the description of interaction between the optical emission and dielectric nanoresonators no simple relationships are used. When it comes to Mie resonances of nanoparticles, an approximate relationship of the observed resonances is often provided (2):

$$\lambda \sim nd, \tag{2}$$

where n is a refraction index, d is a Si NP diameter. Expression (2) matches expression (3):

$$nkr \sim \pi, \tag{3}$$

where k is a wave number, r is a Si NP radius.

As shown in [25], Si NP resonant wavelengths may be also evaluated using a coupled leaking mode theory (CLMT). The optical response in the nanostructure is significantly enhanced, when the incident wavelength matches the leaking modes supported by a nanopillar [25].

Similar to the infinite cylinder leaking modes or confined modes in a strong reflecting end cylinder, relationship (4) is true

$$k_r a = \left((n_{\mathrm{Si}}k)^2 - k_z^2\right)^{1/2} a = K, \tag{4}$$

where k_r is a radial wave vector, k is a free space wave vector, a is a cylinder radius, k_z is a wave vector describing the field amplitude change along the cylinder axis, n_{Si} is the silicon refraction index.

Thus, [26] represents a resonance relationship for mode 1 and mode 2 as follows

$$nkr = K, \tag{5}$$

where $K = 2.6$ is for mode 1 and $K = 5.6$ is for mode 2. According to the simulation, it has been found that the resonant wave length did not substantially depend on the NP height (within 100−215 nm). And the resonance condition was mostly governed by the NP diameter. In [25], for low-order leaking mode resonances for the infinite cylinder with normal lighting $K = 2.31$ and 5.45 ($k_z = 0$). Thus, notwithstanding that the dielectric resonators are generally not described with simple analytical expressions, this equation provides capabilities for identification of Mie resonances.

In equation (5) $K \sim 2.6$ and ~ 5.6, these are constants specific to the observation of Mie resonances in Si NP with a typical height of 272 nm and distance between the adjacent Si NP equal to 188 nm (pitch 460 nm). Also, equation (5) does not include several important factors that influence the initiation of resonances (edge roughness, curvature, taper, etc.). Figure 8 shows the experimental dependence of resonant wavelength vs. the Si NP diameter that was found during our investigation. It is apparent that the reflection minimum position also depends on the Si NP pitch in array.

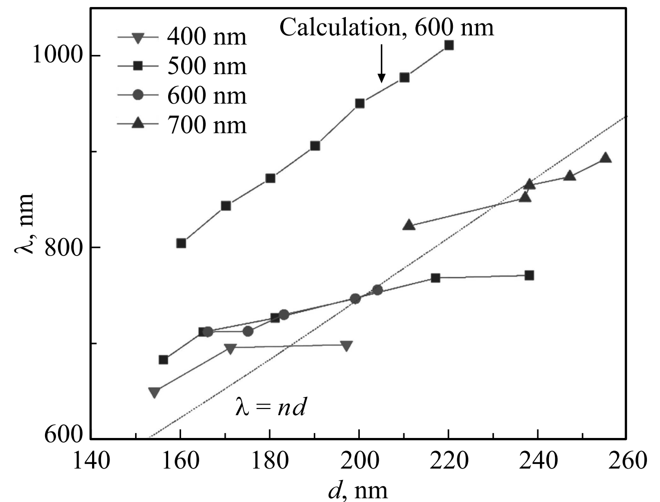

Figure 8. Experimental and calculated dependences of reflection minima positions vs. the Si NP diameter obtained for Si NP with a pitch of 400, 500, 600, 700 nm.

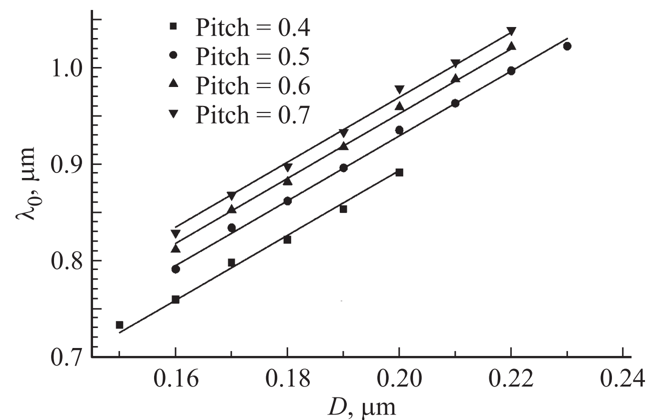

Figure 9. Dependence of absorption maximum position in Si NP for various-pitch square lattice as function of their diameter D. Straight lines are a result of linear approximation with a single slope coefficient 3.365.

The calculation data for similar structures are shown in Fig. 9, where the main minimum position was defined by the maximum absorption spectrum. It can be clearly seen that the peak positions may be described by a straight line with a uniform slope $\kappa = 3.365$ from linear relationship (6):

$$\lambda(D) = \kappa D + B. \tag{6}$$

Coefficient B included in relationship (6) is a fundamental difference of our structures from those described earlier in [25], where the resonance position was approximated by a linear dependence (without offset, i.e. $B = 0$). It shall be noted that the experimental dependences shown in Fig. 8,

also demonstrate a linear dependence of resonance position vs. offset diameter $B \neq 0$.

Thus, based on the shown experimental data and numerical simulation using 3D FDTD method, it may be taken for granted that for Si NP with a height of 450 nm with internal vertical $p-n$-junction formed on a silicon substrate, resonance position is described by an offset linear dependence.

6. Conclusion

Ordered Si NP microarrays that were formed by means of scanning electron lithography on a negative resist with subsequent reactive ion etching have been investigated herein. Si NP had internal vertical $p-n$-junction that was formed on the initial substrate using a molecular beam epitaxy method. The height of Si NP was equal to 450 nm with varying diameter and pitch. It was observed that the light reflection spectra from Si NP were unchanged after Si NP oxidation in concentrated nitric acid. As a result of oxidation in nitric acid, additional passivating coating was removed from the Si NP walls. Numerical simulation of the optical properties corresponded to experimental measurements. Discrepancy between the experimental and calculation results was explained for certain Si NP pitches in array. It was shown that the absorption maximum position dependence for Si NP is of nonzero offset linear type. Alignment of NP with internal $p-n$-junction will further enable to make efficient photodetectors with selectively controlled spectral response curve in a visible and near IR bands.

Appendix

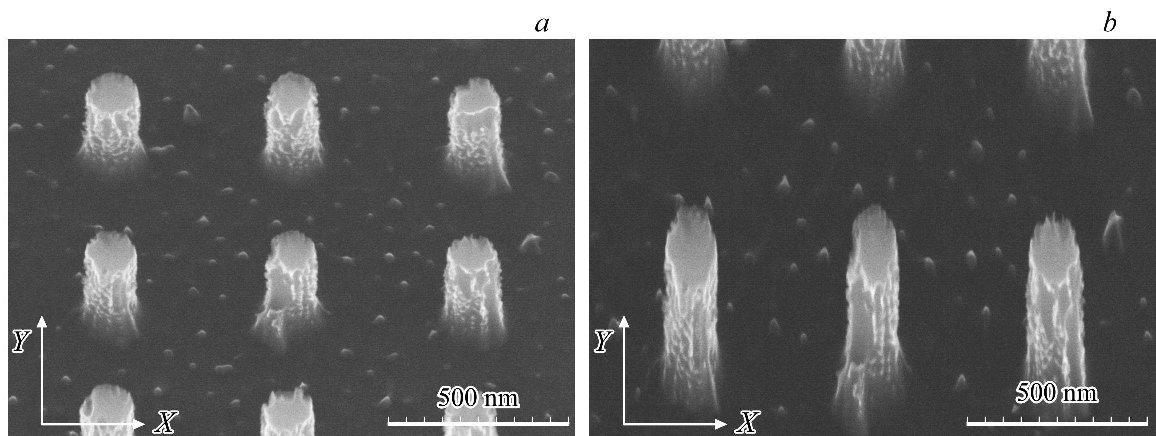

Fig. A.1. SEM image of Si NP, slope angle 30°, without Y axis correction (a) and with Y axis correction (b). Actual height of Si NP is assessed using the figure with Y axis correction, the image without correction is compressed along Y axis.

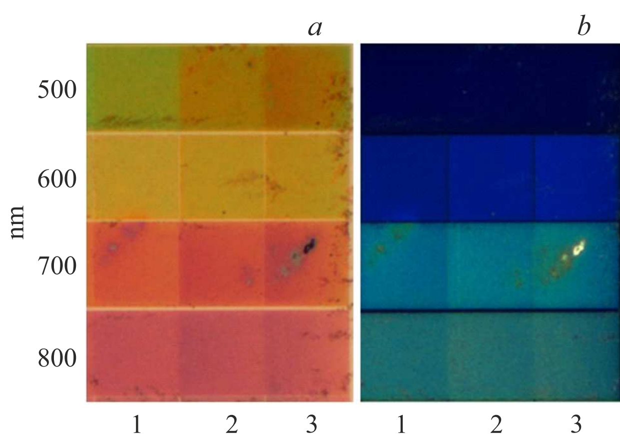

Fig. A.2. Optical images of Si NP arrays in bright field (a) and dark field (b). Pitch 500 nm, diameter: 1) $d = 211\,(181)$ nm, 2) $d = 238\,(217)$ nm, 3) $d = 247\,(238)$ nm; pitch 600 nm, diameter: 1) $d = 211$ (183) nm, 2) $d = 229\,(199)$ nm, 3) $d = 247\,(204)$ nm; pitch 700 nm, diameter: 1) $d = 269\,(238)$ nm, 2) $d = 274$ (255) nm, 3) $d = 287\,(247)$ nm; pitch 800 nm, diameter: 1) $d = 305$ (258) nm, 2) $d = 287\,(270)$ nm, 3) $d = 287\,(258)$ nm.

Funding

Nanostructure forming and diagnostics were supported by the Russian Foundation for Basic Research, grant No. 18-29-20066mk.

Spectroscopic characterization of nanostructures was supported by the Russian Science Foundation (grant No. 17-13-01412).

Acknowledgments

We would like to express deep gratitude for the assistance in the investigations to F.N. Dultsev, PhD in Chemistry, whose life was cut short at the height of his scientific research. Nanostructure forming partially performed using equipment of CKP „Nanostruktury".

Conflict of interest

The authors declare that they have no conflict of interest.

References

[1] Yu. Kivshar. Natl. Sci. Rev., **5** (2) 144 (2018).
[2] Z.-J. Yang, R. Jiang, X. Zhuo, Y.-M. Xie, J. Wang, H.-Q. Lin. Phys. Rep., **701**, 1 (2017).
[3] H. Bertin, Y. Brûlé, G. Magno, T. Lopez, P. Gogo, L. Pradere, B. Gralak, D. Barat, G. Demésy, B. Dagens. ACS Photonics, **5** (7), 2661 (2018).
[4] S.I. Lepeshov, A.E. Krasnok, P.A. Belov, A.E. Miroshnichenko. Phys.-Usp., **61** (11), 1035 (2018).
[5] C. Zou, J. Sautter, F. Setzpfandt, I. Staude. J. Phys. D: Appl. Phys., **52**, 373002 (2019).
[6] K.V. Baryshnikova, M.I. Petrov, V.E. Babicheva, P.A. Belov. Sci. Rept., **6**, 22136 (1–11) (2016).
[7] A. Kuznetsov, A. Miroshnichenko, Y. Fu, J. Zhang, B. Luk'yanchuk. Sci. Rep., **2**, 492 (2012).
[8] V.-C. Su, C.H. Chu, G. Sun, D.P. Tsai. Opt. Express, **26**, 13148 (2018).
[9] M. Brongersma, Y. Cui, S. Fan. Nature Materials, **13**, 451 (2014).
[10] A.L. Hernández, R. Casquel, M. Holgado, I. Cornago, F. Fernández, P. Ciaurriz, F.J. Sanza, B. Santamaría, M.V. Maigler, M. Fe Laguna. Optics Lett., **41** (23), 5430 (2016).
[11] V. Flauraud, M. Reyes, R. Paniagua-Domínguez, A.I. Kuznetsov, J. Brugger. ACS Photonics, **4** (8), 1913 (2017).
[12] H. Li, S. Gao, Y. Li, C. Zhang, W. Yue. Opt. Express, **27** (24), 35027 (2019)
[13] C. Park, V.R. Shrestha, W. Yue, Song Gao, S.-S. Lee, E.-S. Kim, D.-Y. Choi. Sci. Rept., **7** (2556), 1–9 (2017).
[14] W. Yue, S. Gao, S.-S. Lee, E.-S. Kim, D.-Y. Choi. Laser Photonics Rev., **11** (3), 1600285 (2017).
[15] B.-H. Cheong, O.N. Prudnikov, E. Cho, H.-S. Kim, J. Yu, Y.-S. Cho, H.-Y. Choi, S.T. Shin. Appl. Phys. Lett., **94**, 213104, 1 (2009).
[16] X. Li, J. Li, T. Chen, B.K. Tay, J. Wang, H. Yu. Nanoscale Res. Lett., **5**, 1721 (2010).
[17] S. Yalamanchili, H.S. Emmer, K.T. Fountaine, C.T. Chen, N.S. Lewis, H.A. Atwater. ACS Photonics, **3** (10), 1854 (2016).
[18] L.S. Basalaeva, Yu.V. Nastaushev, N.V. Kryzhanovskaya, E.I. Moiseev, D.A. Radnatarov, S.A. Khripunov, D.E. Utkin, I.B. Chistokhin, A.V. Latyshev, F.N. Dultsev. Thin Sol. Films, **672**, 109 (2019).
[19] A. Smyrnakis, P. Dimitrakis, P. Normand, E. Gogolides. Microelectron. Eng., **174**, 74 (2017).
[20] S. Tsoi, F.J. Bezares, A. Giles, J.P. Long, O.J. Glembocki, J.D. Caldwe, J. Owrutsky. Appl. Phys. Lett., **108**, 11110 (1–5) (2016).
[21] N. Dhindsa, R. Kohandani, S.S. Saini. Nanotechnology, **31**, 224001 (2020).
[22] L.S. Golobokova, Yu.V. Nastaushev, F.N. Dultsev, D.V. Gulyaev, A.B. Talochkin, A.V. Latyshev. J. Phys.: Conf. Ser., **541** (1), 012074 (2014).
[23] L.S. Basalaeva, Y.V. Nastaushev, F.N. Dultsev. Materials Today: Proceedings, **4** (11), 11341 (2017).
[24] Rsoft FullWave by SYNOPSYS. Photonic Design Software. https://www.synopsys.com/optical-solutions/rsoft.html.
[25] Y. Yu, L. Cao. Opt. Express, **20**, 13847 (2012).
[26] F.J. Bezares, J.P. Long, O.J. Glembocki, Junpeng Guo, R.W. Rendell, R. Kasica, L. Shirey, J.C. Owrutsky, J.D. Caldwell. Opt. Express, **21** (23), 27587 (2013).